Industrial Robot: An International Journal

Analysis and verification of a miniature dolphin-like underwater glider

Zhengxing Wu Junzhi Yu Jun Yuan Min Tan

Analysis and verification of a miniature dolphin-like underwater glider

Zhengxing Wu, Junzhi Yu, Jun Yuan and Min Tan
Institute of Automation, Chinese Academy of Sciences, Beijing, China

Abstract

Purpose – This paper aims to propose a novel design concept for a biomimetic dolphin-like underwater glider, which can offer the advantages of both robotic dolphins and underwater gliders to achieve high-maneuverability, high-speed and long-distance motions.

Design/methodology/approach – To testify the gliding capability of dolphin-like robot without traditional internal movable masses, the authors first developed a skilled and simple dolphin-like prototype with only gliding capability. The hydrodynamic coefficients, including lift, drag and pitching moment, are obtained through computational fluid dynamics method, and the hydrodynamic analysis in the steady gliding motion is also executed.

Findings – Experimental results have shown that the dolphin-like glider could successfully glide depending on the pitching torques only from buoyancy-driven system and controllable fins without traditional internal moveable masses.

Originality/value – A hybrid underwater glider scheme that combines robotic dolphin and glider is firstly proposed, shedding light on the creation of innovation gliders with maneuverability and durability.

Keywords CFD, Biomimetic robots, Maneuverability, Robotic dolphin, Underwater glider

Paper type Research paper

1. Introduction

Recently, autonomous underwater vehicles (AUVs) are increasingly applied in monitoring aquatic environments in oceans (Williams *et al.*, 2012; Shinzaki *et al.*, 2013; Zhao *et al.*, 2014)[1]. Underwater gliders, as an excellent and typical AUV, have caught much attention in the past three decades because of their astonishing performance such as long distance, extended duration and low cost, which enormously promote the significant and effective applications in huge oceans (Nakamura *et al.*, 2013; Griffiths *et al.*, 2007; Yu *et al.*, 2013).

Traditional underwater gliders usually exploit a skilled buoyancy-driven system to change their volume and buoyancy to ascend and descend in the ocean. Meanwhile, the fixed big-span wings and cylindrical body can result in effective hydrodynamic lift and convert the vertical motion into forward glide. So, the underwater glider can realize a sawtooth motion in the vertical plane and progress along a straight line in the horizontal plane (Zhang *et al.*, 2013; Isa *et al.*, 2014). Moreover, internal moveable masses are usually utilized to regulate the attitude such as pitch and roll angle for a better gliding motion. With a considerable mechanical design and appropriate glide angle control, the buoyancy-driven underwater gliders just consume a minimum power and provide an excellent long-endurance navigation.

Underwater gliding motion was first proposed by Stommel (1989), and then various underwater gliders have been developed and successfully applied in scientific research and ocean observatories such as three great successful commodities – Slocum (Webb *et al.*, 2001), Seaglider (Eriksen *et al.*, 2001) and Spray (Sherman *et al.*, 2001). When orientating the applications in deep oceans, these gliders always adopt special design techniques and could be able to operate in over 1,000-m-deep water and last up to nearly 360 days (Teledyne Webb Research). Because of the relatively little net buoyancy, gliding motion obtains a very low speed and further leads to very limited maneuverability, such as fast turn in minor radius. In some complex aquatic environments, high maneuverability is vital for underwater gliders to fulfill special missions. Consequently, an excellent underwater glider with both great endurance and high maneuverability needed to be developed. Considering dolphins have striking swimming skills in characteristics of high speed, high maneuverability and adaptability, for example, a fast turn with high speed (561.6°/s) (Nagai, 2002; Fish, 2006), we offer a hybrid underwater glider modeled after dolphins.

This paper proposed an innovative design concept for a dolphin-like glider to improve both gliding endurance and maneuverability. As an excellent combination of robotic dolphins and underwater gliders, the dolphin-like underwater glider can not only perform a fast and flexible locomotion in dolphin flapping style but also glide for a long distance depending on its buoyancy-driven system. Besides, owing to its controllable pectoral fins and flattened fluke in horizontal plane, the dolphin-like glider could quickly obtain enough pitching torques to adjust its gliding attitude even without traditional internal moveable masses. Our previous work

The current issue and full text archive of this journal is available on Emerald Insight at: **www.emeraldinsight.com/0143-991X.htm**

Industrial Robot: An International Journal
43/6 (2016) 628–635

[DOI 10.1108/IR-03-2016-0095]

Received 17 March 2016
Revised 4 May 2016
Accepted 6 May 2016

mainly focused on the mechanical design and locomotion control for robotic dolphins (Yu *et al.*, 2011, 2012; 2015). Therefore, we have more confidence in the implementation of dolphin-like motion. By comparison, we care more about the realization of the gliding part in this paper. Consequently, a miniature dolphin-like glider prototype is first developed to testify the glide motion. For a better space utilization rate and drag reduction, the dolphin-like glider adopts a well-streamlined profile from killer whale. A skilled buoyancy-driven system is fixed in the head of the glider to obtain additional pitching torques via absorbing and draining away water. Besides, pectoral fins and flattened fluke could also be manually adjusted for expected pitching torques. The hydrodynamic performance in gliding motion is analyzed by computational fluid dynamics (CFD) method, and key hydrodynamic coefficients, including lift, drag and moment, are also provided for dynamic analysis. The steady gliding motion in the vertical plane is analyzed in detail. Finally, the experiments testified that the dolphin-like glider could successfully glide upward and downward depending on the pitching torques only from buoyancy-driven system and controllable pectoral fins and flattened fluke, even without traditional internal moveable masses.

The rest of this paper is organized as follows. The mechanical design for the simple dolphin-like glider is described in Section 2. The gliding performance analysis using CFD method is detailed in Section 3. Section 4 gives the detailed analysis in the steady gliding motion in the vertical plane. Experimental results and analyses are further offered in Section 5. Finally, Section 6 draws conclusion and presents future work.

2. Mechanical design of the dolphin-like glider

In this section, we will introduce a simple testify dolphin-like underwater glider for gliding motion. As we have confidence and experience in the mechanical design and motion control for a robotic dolphin, the prototype in this paper is only developed to realize gliding motion without dolphin-like dorsoventral joints. Besides, to testify how the pectoral fins and flattened fluke affect the gliding motion, including gliding attitude, gliding speed, etc., controllable pectoral fins and flattened fluke are also designed for the robot. Note that traditional internal moveable masses are specially removed to highlight that the dolphin-like glider could obtain enough pitching torques from internal buoyancy-driven system, controllable pectoral fins and flattened fluke.

The mechanical design of the dolphin-like underwater glider is schematically shown in Figure 1. Generally, the dolphin-like underwater glider is 0.37 m in length and weighs 0.75 kg. A rigid well-streamlined body modeled after killer whale is adopted for a better space utilization rate and lift-drag ratio. The translucent body is made of acrylonitrile butadiene styrene copolymers and could house control circuits, battery packs, gyroscope sensor, communicating modules, buoyancy-driven system, etc. The pectoral fins and flattened fluke, made of polypropylene, can manually be regulated to an expected turn angle via a screw arbor structure. Besides, these fins are specially amplified 1.5 times around the center of the mass for larger pitching torques. The dorsal fin having normal size is fixed on the top for better stability. Specially, these fins adopt

Figure 1 Mechanical design of the miniature dolphin-like glider

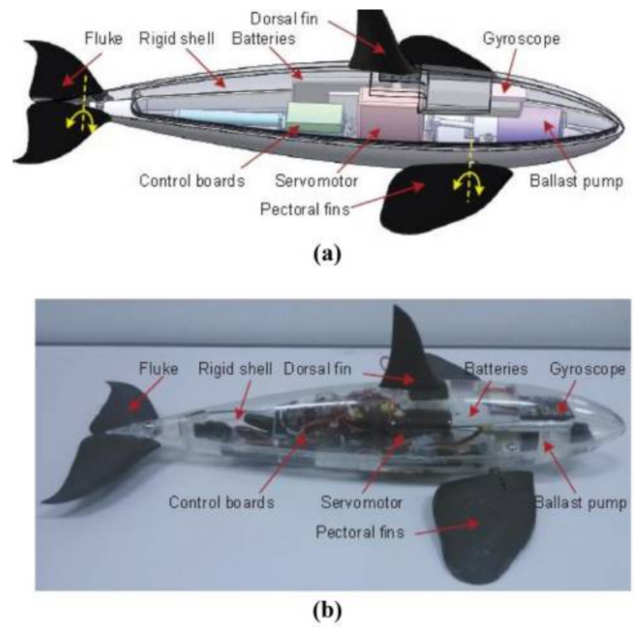

Notes: (a) conceptual design; (b) robotic prototype

a low-speed airfoil, NACA0018, for a better hydrodynamic performance.

To obtain an expected net buoyancy change, the dolphin-like glider adopts a simple and skilled buoyancy-driven system, as shown in Figure 2. Specially, the buoyancy-driven system is composed of an injecting syringe, a waterproof rubber, a digital servomotor and a push-pull structure with an aluminum push rod and a copper rocker. When the servomotor is working, the copper rocker is turned to drive the aluminum push rod to make the rubber move back and forth in the injecting syringe. Meanwhile, the water in injecting syringe changes the buoyancy of the glider to provide the pitching torques for attitude adjustment. Through adjusting the turn angle of the servomotor, the dolphin-like glider could gain an accurate buoyancy change.

3. Computational fluid dynamics simulation and analysis

In this section, we will give a detailed CFD simulation and analysis to explore the gliding performance of the dolphin-like glider and also obtain important hydrodynamic force coefficients.

Figure 2 Mechanical design of the buoyancy-driven system

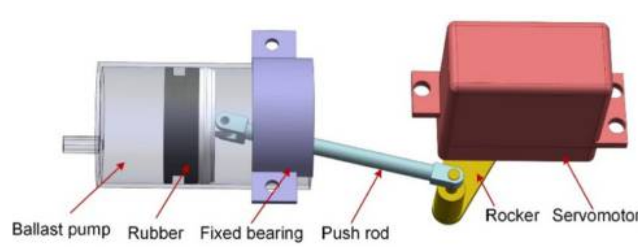

Generally, hydrodynamic force coefficients, such as lift coefficient, drag coefficient and moment coefficient, could be determined using a variety of methods, including airfoil theory, CFD methods and flight tests. Here, CFD methods are used to analyze the gliding performance of the dolphin-like glider. Unlike the fixed wings of traditional underwater gliders, the pectoral fins and flattened fluke of the dolphin-like glider can be manually controlled for expected pitching torques. So, we need to separately compute hydrodynamic coefficients of lifts, drags and pitching moments from dolphin body, pectoral fins and horizontal fluke, which could be applied to the hydrodynamic analysis in glide motion. For an accurate and convenient CFD simulation results, the commercial software Analysis System is used (ANSYS Inc.). Specially, ICEM CFD software is adopted as the pre-processing tool to build a mesh for the glider which forms the finite flow domain, and Fluent is applied to simulate the flow and pressure distribution around the glider when it is in motion.

In the following, we take the dolphin body, for example, to introduce the whole CFD simulation process. For the pectoral fins and flattened fluke, the CFD simulations adopt similar settings. In the pre-processing meshing work, an unstructured tetrahedron mesh is formed to describe the flow domain for great adaptability and high quality, as shown in Figure 3. The whole computation domain of the dolphin body is surrounded by the following boundaries:

- *Inlet boundary*: It is two times body lengths from the nose and is set as velocity-inlet with $v = 0.1$ m/s.
- *Outlet boundary*: It is three times body lengths from the fluke and is set as outflow.
- *Top and bottom boundaries*: It is set as velocity-inlet as $v = 0.1$ m/s to avoid reflected effects.
- *Far field boundary*: It is set as no-flip walls.
- *Surface boundary*: It is set as no-slip moving walls.

Meanwhile, for better simulation results, seven prismatic layers are stacked onto the surface mesh, as shown in Figure 4(a) and (b). The CFD simulations about the pectoral fins and flattened fluke adopt the similar boundary conditions, and also several prismatic layers, as shown in Figure 4(c) and (d). In addition, the fluid is supposed as to be an incompressible and steady one, and *k-w* shear-stress-transport

Figure 3 Boundary conditions for the dolphin-like glider

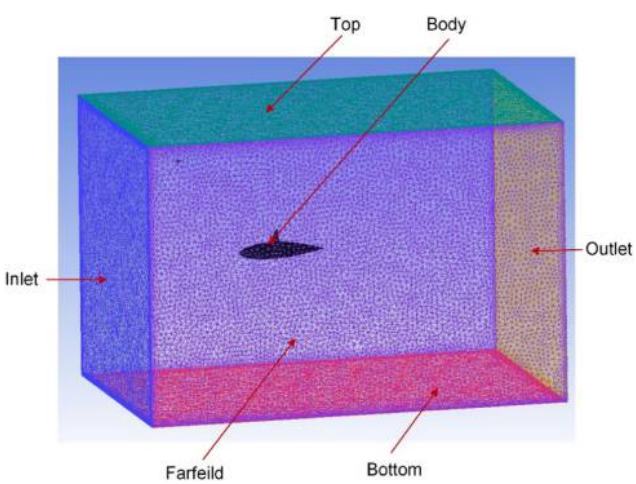

Figure 4 Unstructured tetrahedron mesh of dolphin-like glider

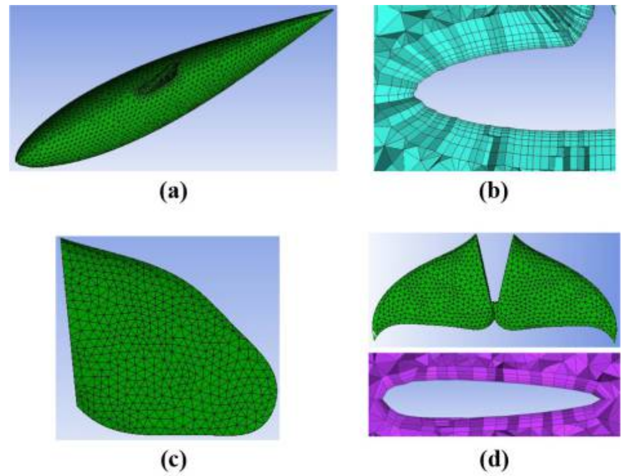

Notes: (a) surface mesh of the body; (b) cut-plan of volume mesh around the cylindrical body; (c) surface mesh of the pectoral fin; (d) surface mesh of the flattened fluke and cut-plan of volume mesh around the flattened fluke

turbulence model with low-Re corrections are adopted in Fluent simulation.

When gliding steadily in the vertical plane, the hydrodynamic force coefficients could be simplified as a function about the angle of attack, for example, monomial for lift coefficient and moment coefficient and quadratic polynomial for a drag coefficient, according to the previous results (Leonard and Graver, 2001; Zhang *et al.*, 2013; Fan and Craig, 2014). For the dolphin-like glider, the asymmetric body shape leads to a slightly more complex relationship between the hydrodynamic coefficients and angle of attack. According to the simulation results, we found that quartic polynomial is much better than quadratic polynomial or monomial to fit the curves of the hydrodynamic coefficients of the dolphin body, as shown in Figure 5(a)-(c). For the pectoral fins and flattened fluke, the quadratic polynomial and monomial could obtain an expected fitting result, as shown in Figure 5(d)-(f). According to these CFD simulation results mentioned above, we can obtain the hydrodynamic coefficients about the dolphin body, pectoral fins and flattened fluke as follows:

$$\begin{cases} C_{D_{body}}(\alpha) = 6.489\alpha^4 + 0.0502\alpha^3 + 1.212\alpha^2 \\ \qquad - 0.02245\alpha + 0.2588 \\ C_{L_{body}}(\alpha) = 0.5397\alpha^4 + 8.302\alpha^3 - 0.1858\alpha^2 \\ \qquad + 0.7755\alpha - 0.01042 \\ C_{M_{body}}(\alpha) = 0.3971\alpha^4 + 0.4672\alpha^3 - 0.02648\alpha^2 \\ \qquad - 0.214\alpha + 0.0011 \end{cases}, \quad (1)$$

$$\begin{cases} C_{D_{pec}}(\alpha) = 1.481\alpha^2 - 0.000357\alpha + 0.6758 \\ C_{L_{pec}}(\alpha) = 1.667\alpha - 0.003487 \\ C_{M_{pec}}(\alpha) = -0.09995\alpha + 0.0009239 \end{cases}, \quad (2)$$

Figure 5 Hydrodynamic coefficients over the angle of attack of the dolphin body and pectoral fins

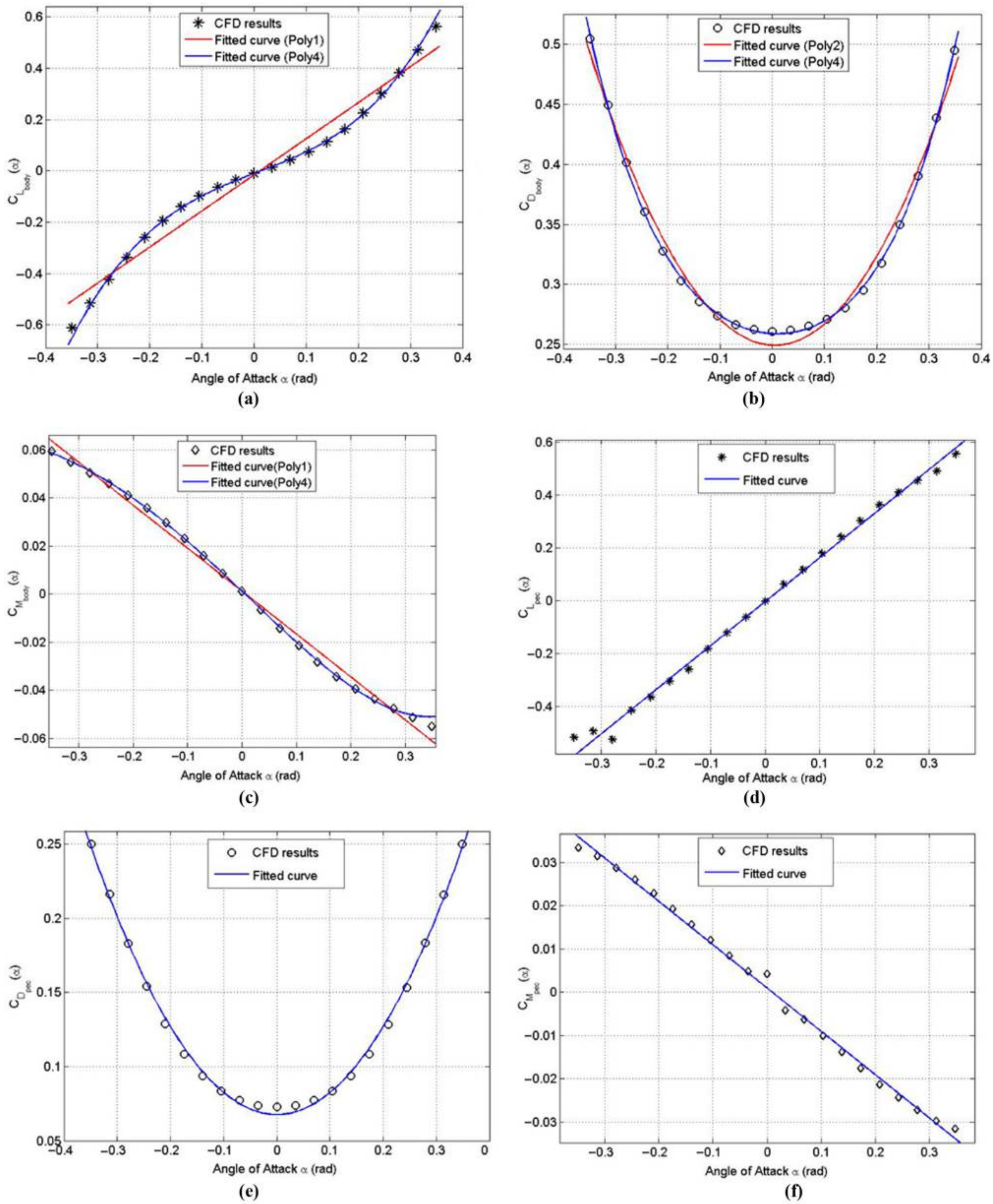

Notes: (a) lift coefficient of the dolphin body; (b) drag coefficient of the dolphin body; (c) pitching moment coefficient of the dolphin body; (d) lift coefficient of the pectoral fin; (e) drag coefficient of the pectoral fin; (f) pitching moment coefficient of the pectoral fin

$$\begin{cases} C_{D_{fluke}}(\alpha) = 1.344\alpha^2 - 0.002419\alpha + 0.09103 \\ C_{L_{fluke}}(\alpha) = 1.601\alpha \\ C_{M_{fluke}}(\alpha) = 0.3446\alpha - 0.000524 \end{cases}, \quad (3)$$

where C_{D_i}, C_L, C_M (i = *body*, *pec*, *fluke*) separately respect the hydrodynamic drag, lift and moment coefficients by cross-sectional area for dolphin body, pectoral fins and flattened fluke, respectively.

The analysis in the dynamic and static pressure distribution around the dolphin-like glider is also executed. Figure 6 separately displays these pressure distributions around the glider. We can see that the highest pressure is at the tip of the glider's nose and the windward side of every fin or fluke, because of the interaction between the fluid and the dolphin-like glider. These pressures on the rest of the glider surface are both lower because of the smooth flow. Generally, these pressures are all too small to be sustainable and do not cause any destruction effect for the dolphin-like glider.

4. Analysis of the steady gliding motion

In this section, a detailed hydrodynamic analysis for the dolphin-like glider during a steady gliding motion is presented. Note that the dolphin-like glider has the controllable pectoral fins and flattened fluke, which could change the hydrodynamic performance through adjusting their turning angles. Therefore, hydrodynamic forces on the dolphin body, pectoral fins and the flattened fluke should be separately analyzed, which are different from those on the traditional gliders (Leonard and Graver, 2001; Fan and Craig, 2014).

Figure 7 defines the coordinate frames, including an inertial frame and a body reference frame, to describe the gliding motion. In the inertial frame E_{xyz}, the horizontal axes of X and Y are perpendicular to the gravity, and the Z-axis is along the positive gravity direction. Note that the inertial frame is considered to be earth-fixed and no-rotating. For the body reference frame O_{xyz}, the coordinate center is fixed in the center of buoyancy of the glider, the x-axis is along the longitudinal axis of the dolphin-like glider from fluke to head, the y-axis is along the pectoral shafts from left to right and the z-axis follows the right-hand rule. Let R and b denote the rotation matrix from the body frame to the inertial frame and the vector from the origin of the inertial frame to the origin of the body frame, respectively.

To obtain the hydrodynamic performance in a steady gliding motion, we first suppose that the dolphin-like glider gets hydrodynamic equilibrium in the vertical plane. Therefore, it is easy to get the vertical plane equilibrium equations as follows:

$$\begin{aligned} \dot{x} &= v_x \cos\theta + v_z \sin\theta \\ \dot{z} &= -v_x \sin\theta + v_z \cos\theta \\ 0 &= (m_z - m_x)v_x v_z - m_b g(r_{b_z}\cos\theta + r_{b_x}\sin\theta) + M_{DL_{Total}}, \\ 0 &= -m_0 g \sin\theta + L_{Total_x} + D_{Total_x} \\ 0 &= m_0 g \sin\theta + L_{Total_z} + D_{Total_z} \end{aligned} \quad (4)$$

where v_x and v_z are, respectively, the components of the gliding velocity in the x- and z-directions; θ denotes the pitch angle of the robotic dolphin; m_0 and m_b are, respectively, the net buoyancy of the glider and the variable ballast point mass, which is offset r_b from the center of buoyancy; m_x and m_z are, respectively, the added mass terms corresponding to the x- and z-directions; and L_{Total_x}, L_{Total_z}, D_{Total_x}, D_{Total_z}, $M_{DL_{Total}}$ are,

Figure 6 Pressure contour of the dolphin-like glider

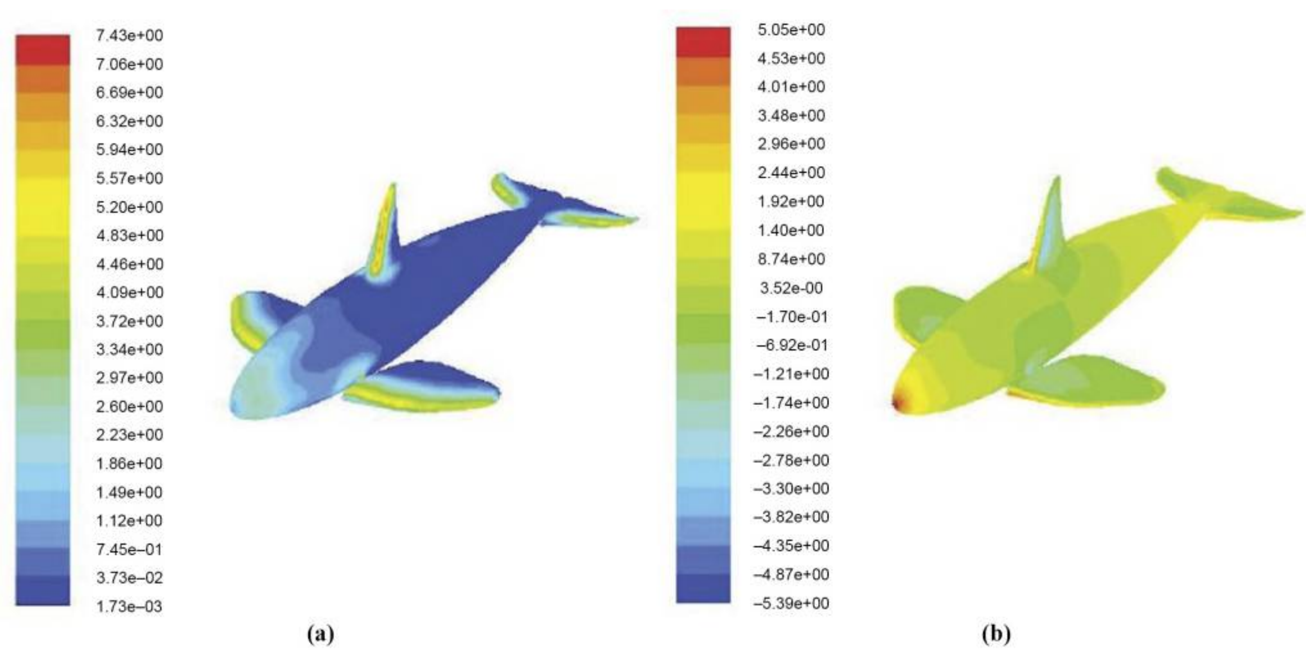

Notes: (a) dynamic pressure; (b) static pressure

Figure 7 Coordinate systems defined to describe the steady gliding motion

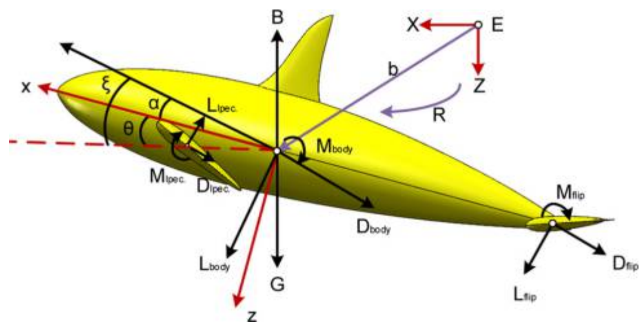

respectively, the sum of the hydrodynamic forces on the body, pectoral fins and fluke, as shown in the following equations:

$$\begin{array}{rcl} L_{Total_x} & = & (L_{body} + L_{lpec} + L_{rpec} + L_{fluke})\sin\alpha_{body} \\ L_{Total_z} & = & -(L_{body} + L_{lpec} + L_{rpec} + L_{fluke})\cos\alpha_{body} \\ D_{Total_x} & = & -(D_{body} + D_{lpec} + D_{rpec} + D_{fluke})\cos\alpha_{body} \\ D_{Total_z} & = & -(D_{body} + D_{lpec} + D_{rpec} + D_{fluke})\sin\alpha_{body} \\ L_i & = & 0.5\rho C_{L_i}(\alpha_i)S_i v^2 \\ D_i & = & 0.5\rho C_{D_i}(\alpha_i)S_i v^2 \end{array}, \quad (5)$$

where i = body, lpec, repc and fluke denotes the related variable about the dolphin body, left pectoral fin, right pectoral fin and flattened fluke; L_i, D_i, respectively, denote the hydrodynamic lift and drag on the body, left pectoral fin, right pectoral fin and flattened fluke; α_i indicates the angle of attack of the glider; α_i (i = lpec, repc and fluke) can be obtained through α_{body} and turn angles of pectoral fins and fluke; s_i denotes the maximum cross-sectional area; ρ indicates the fluid density; and ν denotes the relative velocity of the robotic dolphin with respect to the fluid:

$$\theta = \arctan\left(-\frac{\sum C_{L_i}(\alpha_i)\sin\alpha_{\mathrm{body}} - \sum C_{D_i}(\alpha_i)\cos\alpha_{\mathrm{body}}}{\sum C_{L_i}(\alpha_i)\cos\alpha_{\mathrm{body}} - \sum C_{D_i}(\alpha_i)\sin\alpha_{\mathrm{body}}}\right). \quad (6)$$

According to the equilibrium equations, we easily obtain the relationship between pitch angle θ and the angle of attack α_i for the dolphin-like glider, as shown in equation (6). We can find that the pitch angle θ only depends on the angle of attack α_i, the lift coefficient, drag coefficient of the dolphin body, pectoral fins and flatten fluke and is independent of the others. Therefore, we can easily control the pitch angle θ or the angle of attack α of the gliding robotic dolphin for an expected gliding motion through adjusting the turn angle β_i of pectoral fins and flatten fluke. Figure 8 depicts the pitch angle θ varying with the angle of attack of the body α_i with different turn angle β_i. According to the black and green curves in Figure 8, we can see that a little adjustment for β_{pec}, about 5°, even with $\beta_{fluke} = 0°$, could successfully lead to an expected pitch angle θ. If we also adjust β_{fluke} at the same time, more apparent effects can be achieved (see the red and blue curves in Figure 8). These results illustrate that the controlled pectoral fins and flattened fluke will bring obvious effects for adjusting gliding attitude.

5. Experiments and discussion

To evaluate the gliding performance of the dolphin-like glider, extensive experiments have been carried out. These experiments were conducted in an indoor water tank with a dimension of 1.9 × 1.0 × 0.8 m. During these experiments, unless otherwise specified, the data points and error bars in figures were the averages and standard deviations of three runs, respectively.

The first experiment focused on the downward gliding motion. At the beginning, the dolphin-like glider got a force balance in the surface of the water, as shown in Figure 9(a). When receiving the descending command from computer, the dolphin-like glider absorbed about 4.6 g water to change its buoyancy and started to glide downward (Figure 9(b)–(i)). To explore how the angle affected the glide speed, the turn angle β between pectoral fins and body was manually changed from 0° to 15° every 5°. Figure 10 gives the relationship between downward gliding velocities and the turn angle of pectoral fins. From Figure 11, we can see that the dolphin-like glider gained the highest horizontal speed of 9.56 cm/s when $\beta = -10°$ and the highest vertical speed of 7.97 cm/s when $\beta = -15°$.

The second experiment was carried out to testify the upward gliding motion. Similar to downward glide, the upward gliding motion could be successfully realized through draining away 4.6 g water, as shown in Figure 11. According to the experimental results, we can see that the dolphin-like glider could obtain the highest horizontal speed of 6.27 cm/s when $\beta = 5°$ and the highest vertical speed of 4.96 cm/s when $\beta = 15°$. We can see that the dolphin-like glider had different vertical speeds in upward and downward gliding motion, although β had the same value (–15° and 15°). This phenomenon is mainly due to the asymmetric body shape of the dolphin-like glider, which leads to different hydrodynamic performances such as different pitch angles and gliding path angles in upward gliding motion and downward gliding motion. Therefore, the dolphin-like glider obtained different vertical speeds in upward and downward gliding motions, although the turn angles of pectoral fins had the same value (–15° and 15°) (Figures 11 and 12).

Traditional underwater gliders usually use the internal moveable masses to regulate the gliding attitude. Because of back and forth movements, the internal masses often occupy large space that leads to a low space utilization rate. Comparatively, the dolphin-like glider provided in this paper could obtain enough pitching torques from both buoyancy-driven system and controllable fins, including pectoral fins and flattened fluke. Moreover, the fluke often provides a considerable pitching moment because of the relative larger moment arm. In this situation, the buoyancy-driven system only needs a little volume for water, about ±0.6 per cent of the whole displacement. The volume of the buoyancy-driven system and turn angle of the controllable fins could also be used as controlled input variables for an expected accurate attitude. Moreover, flexible pectoral fins and flattened fluke could bring quick response capability into the attitude adjustment.

6. Conclusions and future work

In this paper, we have provided a novel design concept of a dolphin-like glider. To testify and analyze the gliding motion without the traditional internal moveable masses, a miniature dolphin-like glider prototype has been developed. With the help

Figure 8 The relationship between pitch angle θ and the angle of attack α_i

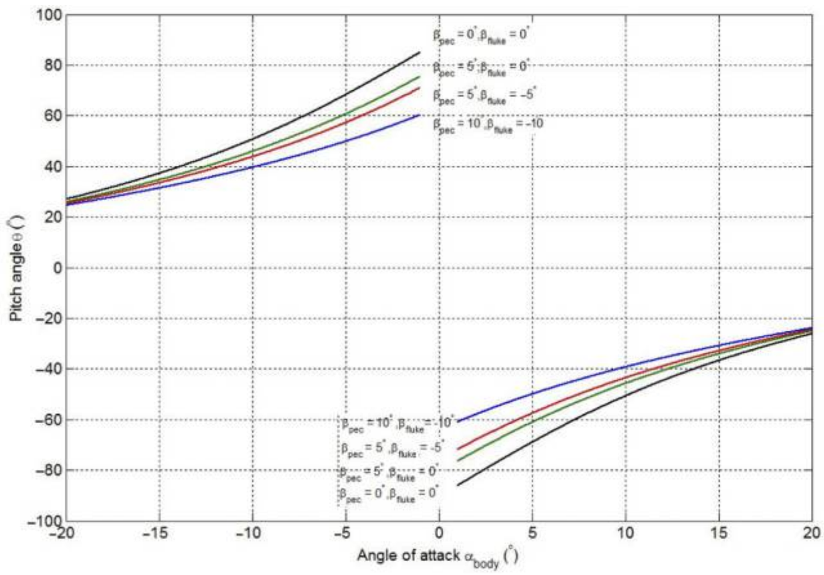

Figure 9 Snapshot sequence of downward gliding motion

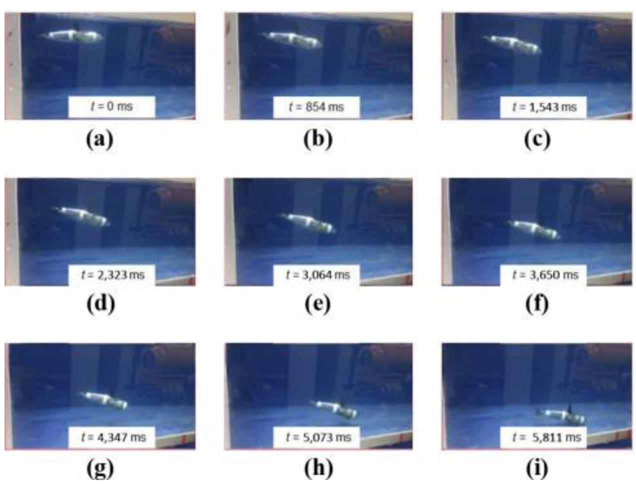

Figure 10 The relationship between downward gliding velocities and the turn angle of pectoral fins

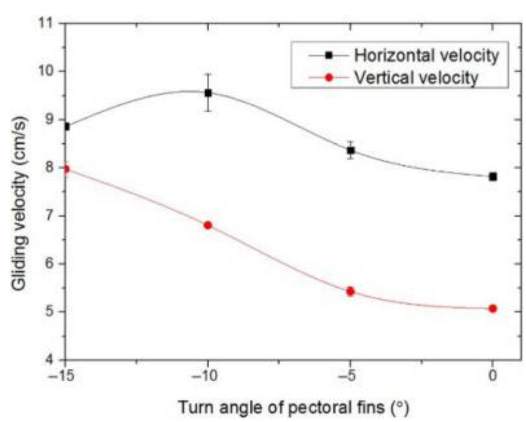

Figure 11 Snapshot sequence of upward gliding motion

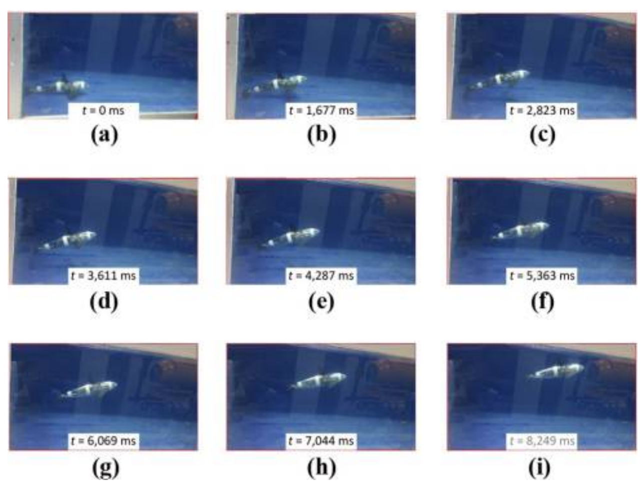

Figure 12 The relationship between upward gliding velocities and the turn angle of pectoral fins

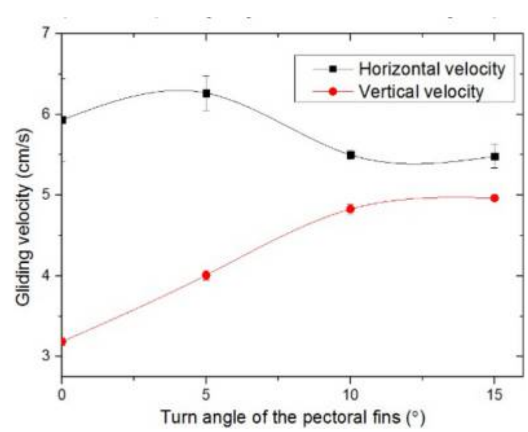

of CFD simulation, the hydrodynamic characteristics in gliding motion have been analyzed, and important hydrodynamic coefficients over the angle of attack and pressure distribution have also been provided for the following dynamic analysis. Experimental results verify that the dolphin-like glider could successfully glide upwards and downwards relying on the pitching torques only from buoyancy-driven system and controllable pectoral fins and flattened fluke, even without traditional internal moveable masses.

The ongoing and future work will focus on the mechanical design and motion control for a real dolphin-like underwater glider possessing both dolphin-like swimming and quiet gliding motion. Thus, the biomimetic underwater glider could show excellent performance with high maneuverability and long endurance.

Note

1. This work was supported in part by the National Natural Science Foundation of China (No. 61375102, No. 61333016 and No. 61421004), the National Defense Science and Technology Innovation Found of Academy of Sciences (No. CXJJ-16M110), the Beijing Natural Science Foundation (No. 4164103 and No. 3141002) and the Early Career Development Award of SKLMCCS.

References

Eriksen, C.C., Osse, T.J., Light, R.D., Wen, T., Lehman, T.W., Sabin, P.L., Ballard, J.W. and Chiodi, A.M. (2001), "Seaglider: a long-range autonomous underwater vehicle for oceanographic reaearch", *IEEE Journal Oceanic Engineering*, Vol. 26 No. 4, pp. 424-436.

Fan, S. and Craig, A.W. (2014), "Dynamics of underwater gliders in currents", *Ocean Engineering*, Vol. 84, pp. 249-258.

Fish, F.E. (2006), "Drag reduction by dolphins: myths and reality as applied to engineered designs", *Bioinspiration & Biomimetics*, Vol. 1 No. 1, pp. R17-R25.

Griffiths, G., Jones, C., Ferguson, J. and Bose, N. (2007), "Undersea glider", *Journal of Ocean Technology*, Vol. 2 No. 2, pp. 64-75.

Isa, K., Arshad, M.R. and Ishak, S. (2014), "A hydrid-driven underwater glider model, hydrodynamics estimation, and an analysis of the motion control", *Ocean Engineering*, Vol. 81 No. 1, pp. 111-129.

Leonard, N.E. and Graver, J.G. (2001), "Model-based feedback control of autonomous underwater gliders", *IEEE Journal of Oceanic Engineering*, Vol. 26 No. 4, pp. 633-645.

Nagai, M. (2002), *Thinking Fluid Dynamics with Dolphins*, Ohmsha, Tokyo.

Nakamura, M., Asakawa, K., Hyakudome, T., Kishima, S., Matsuoka, H. and Minami, T. (2013), "Hydrodynamic coefficients and motion simulations of underwater glider for virtual mooring", *IEEE Journal of Oceanic Engineering*, Vol. 38 No. 3, pp. 581-597.

Sherman, J., Davis, R.E., Owens, W.B. and Valdes, J. (2001), "The autonomous underwater glider 'Spray'", *IEEE Journal Oceanic Engneering*, Vol. 26 No. 4, pp. 437-446.

Shinzaki, D., Gage, C., Tang, M., Wolfe, B., Lowe, C.G. and Clark, C. (2013), "A multi-AUV system for cooperative tracking and following of leopard sharks", *Proceedings of the IEEE International Conference on Robotics and Automation*, IEEE, *Karlsruhe*, 6-10 May, pp. 4153-4158.

Stommel, H. (1989), "The slocum mission", *Oceanography*, Vol. 2 No. 1, pp. 22-25.

Webb, D.C., Simonetti, P.J. and Jones, C.P. (2001), "SLOCUM: an underwater glider propelled by environmnetal energy", *IEEE Journal of Oceanic Engineering*, Vol. 26 No. 4, pp. 447-452.

Williams, S.B., Pizarro, O.R., Jakuba, M.V. and Johnson, C.R. (2012), "Monitoring of benthic reference sites: using an autonomous underwater vehicle", *IEEE Robotics and Automation Magazine*, Vol. 19 No. 1, pp. 73-84.

Yu, J., Su, Z., Wang, M., Tan, M. and Zhang, J. (2012), "Control of yaw and pitch maneuvers of a multilink dolphin robot", *IEEE Transactions on Robotics*, Vol. 28 No. 2, pp. 318-329.

Yu, J., Su, Z., Wu, Z. and Tan, M. (2015), "An integrative control method for bio-inspired dolphin leaping: design and experiments", *IEEE Transactions on Industrial Electronics*, Vol. 63 No. 5, pp. 3108-3116.

Yu, J., Wang, M., Tan, M. and Zhang, J. (2011), "Three-dimensional swimming", *IEEE Robotics and Autonomous Magazine*, Vol. 18 No. 4, pp. 47-58.

Yu, J., Zhang, F., Zhang, A., Jin, W. and Tian, Y. (2013), "Motion parameter optimization and sensor scheduling for the sea-wing underwater glider", *IEEE Journal of Ocean Engineering*, Vol. 38 No. 2, pp. 243-254.

Zhang, S., Yu, J., Zhang, A. and Zhang, F. (2013), "Spiraling motion of underwater gliders: modeling, analysis, and experimental results", *Ocean Engineering*, Vol. 60 No. 1, pp. 1-13.

Zhao, B., Skjetne, R., Blanke, M. and Dukan, F. (2014), "Particle filter for fault diagnosis and robust navigation of underwater robot", *IEEE Transactions on Control Systems Technology*, Vol. 22 No. 6, pp. 2399-2407.

Further reading

ANSYS Inc (2016), available at: www.ansys.com/ (accessed 29 April 2016).

Teledyne Webb Research (TWR) (2016), available at: www.webbresearch.com/slocumglider.aspx (accessed 29 April 2016).

Corresponding author

Zhengxing Wu can be contacted at: zhengxing.wu@ia.ac.cn